Wasit Journal of Engineering Sciences
Journal homepage: https://ejuow.uowasit.edu.iq
Vol. 14 No. 2 June 2026, pp.468-476
https://doi.org/10.31185/ejuow.v14i2.883

ISSN 2305-6932
Original Research

Experimental Temperature Measurements on a Full-Scale Reinforced Concrete Box-Segment during the Construction Stage

Noora K. Jebur[1], Sallal R. Abid[1], Mustafa Özakça[2]

[1]Department of Civil Engineering, College of Engineering, Wasit University, Iraq
[2]Department of Civil Engineering, College of Engineering, Gaziantep University, Turkey

Corresponding Author Email: ***Std2024203.m.kar@uowasit.edu.iq***

Received Jan.24, 2026 | Revised Apr.10, 2026 | Accepted. May.23, 2026 | Online Jun.1, 2026

ABSTRACT

A full-scale square-hollow reinforced concrete segment was constructed in an open environment to evaluate the effect of the heat produced from cement hydration and the environmental cycles of cooling and heating during the first 48 hours on concrete after casting. Totally, ten thermocouples were installed in the segment, where eight thermocouples were installed along the centreline of four walls, where the wall thickness was 500 mm, while two more thermocouples were installed at the exterior and interior wall surfaces. Three environmental sensors were also installed at the site to measure air temperature, solar radiation, and wind speed. The results showed that minor differences were recorded between the eight thermocouples during the first 24 hours, while the southwest thermocouple recorded temperatures that were slightly higher during the day and slightly lower during the night compared to the core thermocouples, revealing some sensitivity to environmental thermal loads. The comparisons of the first 48 hours' temperatures with those after 72 hours showed that the hydration heat increased the concrete temperature by approximately 26 to 32 ^{o}C during the first 24 hours. Additionally, the effect of hydration heat became minimal after 30 hours and diminished after 36 hours, which declares the start of the life-span state of full-dependency on solar radiation and air temperature.

Keywords: Concrete temperature; early age; temperature distribution; solar radiation; air temperature; hollow-concrete section

1. Introduction

The hydration of concrete generates considerable heat during the first few days, where the emission of heat may cause high temperatures in the mass core because of the thermal insulation effect of molds and the low thermal conductivity of concrete [1]. The daily variations in air temperature and solar radiation add an extra thermal challenge during the early age period, where the combined influence of external thermal stresses and hydration heat-induced stresses could result in serious early-age cracking [2, 3]. Keeping in mind that Ordinary Portland cement can release up to 500 joules of heat per gram as a result of cement hydration [4], after reaching its maximum, the time-dependent drop of concrete temperature depends on several parameters, including the amount of forming sealant, area of open-air surfaces where convection occurs, air temperature, and wind speed. These parameters affect how much heat is dissipated from concrete interiors to the surrounding atmosphere via open surfaces. Heat leakage into the surrounding environment causes the concrete's surface temperatures to drop, resulting in nonlinear temperature gradients [5], which induce stresses and deformations in restricted and unrestricted structures [6]. Additionally, cracking typically happens in early concrete structures when surface tensile stresses surpass the concrete's overall tensile strength, which is still lower than its target mature strength [7]. This problem must be thoroughly evaluated during the construction of concrete bridge superstructures, piers, and pylons due to their typically large volume [8].

Most of the previous studies focused on temperature variations and gradients in bridge superstructures. Chen et al. [9] examined the thermal behavior and thermal stresses in prestressed concrete box girders through

continuous field measurements, emphasizing the effects of cement hydration heat and solar radiation. The findings demonstrated that there is a quasi-linear relationship between the casting temperature and the maximum temperature attained within the section, and that significant temperature disparities between the center and surface of the section result in thermal tensile strains that may induce premature thermal cracking. They also reported that solar radiation produces nonlinear thermal gradients and thermal stresses that may exceed those caused by live loads. Abid et al. [10] constructed a full-scale concrete box-girder instrumented with several temperature sensors to evaluate the effect of early age hydration heat on bridge structures. Laibi and Shallal [11] constructed a similar experimental work on a T-concrete girder segment for the same purpose. Both research works revealed similar conclusions to those reported by Chen et al. [9]. Zhang et al. [12] examined the influence of hydration heat on the thermal and structural performance of composite concrete-filled steel towers utilizing field measurements. The temperature measurements showed that the tower's interior temperature exceeded 70°C with significant temperature gradients between the core and the top surface, which increased the risk of cracking. Phung and Nguyen [13] examined the thermal field in concrete bridge piles during construction by the finite element method. They reported that premature thermal cracking is more likely when the cement content and casting temperature are raised due to the increased temperature gradient between the core and surfaces of the pile. The study also showed that because wooden formwork has a lower thermal conductivity than steel formwork, it lowered the thermal gradient.

The purpose of this work is to investigate the early-age temperature gradients in hollow vertical concrete structural elements caused by the interaction of hydration heat and ambient thermal stress. Temperature sensors were placed at along the concrete core perimeter and a corner section of a hollow-core square reinforced concrete structural segment located in an open field to achieve this purpose. In the same field, a climatic monitoring system was also installed to monitor the environmental thermal loads during the first few days of construction. The study presents field-measured temperature distributions, which can serve as an experimental basis for assessing how early-age thermal loads affect the structural response of large hollow reinforced concrete structural members, such as bridge piers.

2. Experimental Work

To investigate temperature distributions and differences in concrete bridges under environmental conditions, a 2.5 m-high and 2.1 m-wide full-scale hollow reinforced concrete box-segment with 0.5 m wall thickness was constructed in an open area to replicate the bridge pier construction stage. A plywood formwork was used to cast the segment, as shown in Figure 1(a), while a shallow concrete base was cast a few days before to facilitate the casting and instrumentation of the box segment. Because the segment is not intended to be tested under any sort of mechanical loads, and to control temperature-related shrinkage cracking, two layers of vertical and horizontal (exterior and interior) 10 mm-diameter reinforcing bars were used as main reinforcement, while a C40 conventional concrete was supplied from a neighboring ready-mix concrete mixer to pour the concrete of the segment.

Ten thermocouples were used to measure the concrete's temperatures. The thermocouples were separated into eight locations at the center of the wall thickness (N, S, NE, NW, SE, SW, W, and E), while the other two thermocouples were placed at the inner and outer edges of the wall thickness along the southwest direction corner-section of the segment (SWint and SWext.). Depending on the solar movement to the south of the equator during this period of the year, the SW corner is much affected by solar radiation compared to the other corner, where it receives radiation from the south along the late hot-morning hours, noon hours, and the effective afternoon hours from the west side, which the reason behind selecting this corner to install the surface thermocouples. Figure 1(b) shows the thermocouple distribution and the sectional geometry of the box-segment. An effective weather station with three thermocouples was also installed near the experimental box-segment, which included a pyranometer to record the solar radiation intensity variation with time, an anemometer used for recording wind speed variation, and an air temperature probe to capture the time-dependent variation of air temperature. A reliable and compatible Campbell Scientific® data acquisition system was deployed to read and record all measurements at constant time steps of 30 minutes during the first 48 hours, starting from the time of concrete casting.

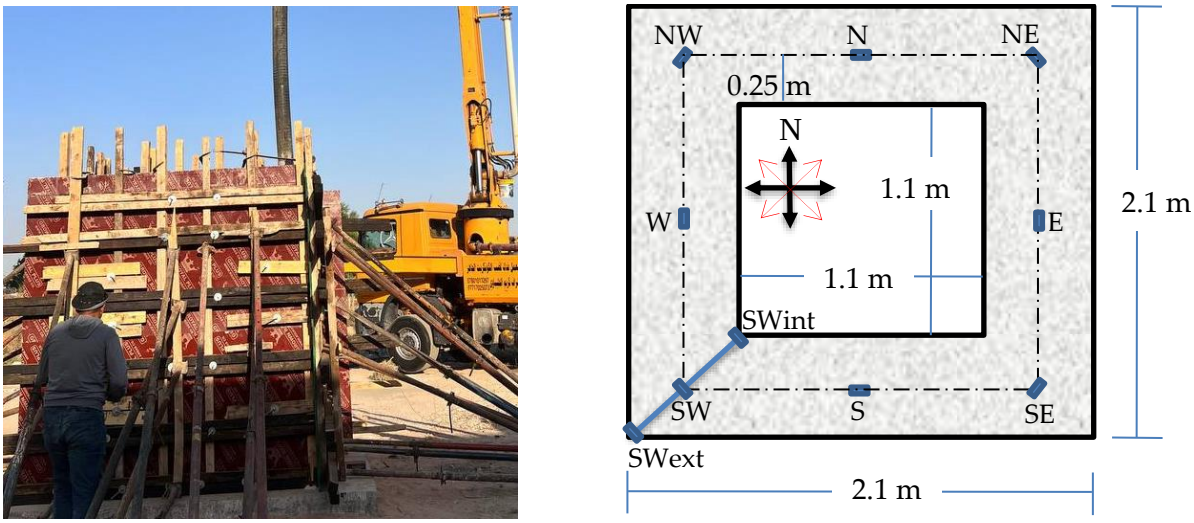

Figure 1. The experimental box-segment (a) formwork and construction (b) geometry and temperature sensors

3. Results & Discussion

3.1 Air temperature, solar radiation, and wind speed

Since the box-segment was constructed in an open environment, it was directly and openly exposed to the atmospheric variation of air temperature, solar radiation, and wind speed. Thus. A better understanding of concrete temperature variation requires an adequate knowledge of the time-dependent alteration of these environmental thermal loads. The recorded environmental thermal loads during the investigated 48 hours are presented in Figure 2. As shown in Figure 2(a), the temperature at casting time (2:30 PM) was 37.1 ^{o}C, which continued decreasing during the rest of the day hours, due to the decline of solar radiation shown in Figure 2(b), and during the night hours to reach a minimum of 23.9 ^{o}C at approximately 5:30 AM. As with the early shining hours, the solar radiation heating phase started at approximately 6:00 AM (Figure 2(b)), the air temperature started its next day's ascending response up to reaching its maximum records within the mid-day hours, where the maximum recorded air temperature of the next day was slightly higher than 40 ^{o}C, which was recorded at 2:00 PM, which was occurred 2 hours after recording a daily maximum hourly solar radiation of 825 W/m^2. The same sequence of night-decrease and day-increase of air temperature continued along the third day, but with different daily maximum and minimum temperatures of 38 ^{o}C and 23.5 ^{o}C, respectively.

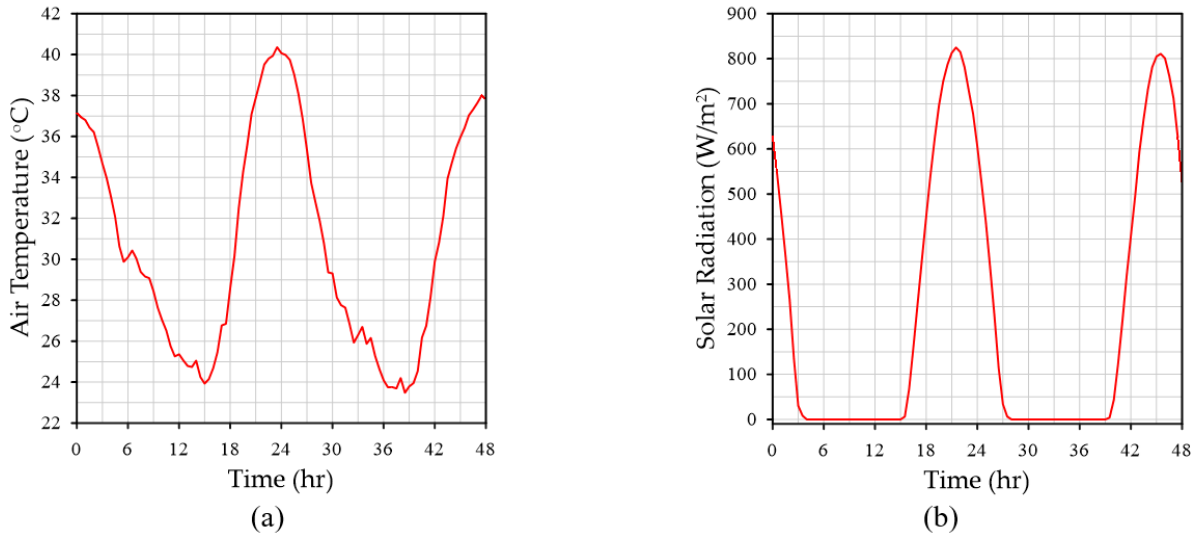

Figure 2. Hourly atmospheric thermal loads (a) air temperature (b) solar radiation (c) wind speed

It is obvious from Figure 2(b) that the sky was free of any cloud cover during the three investigated days, where there are no fluctuations in the solar radiation wave. The maximum hourly solar radiation of the third day was 811 W/m^2, which was also recorded at midday. Figure 2(c) shows that the wind speed mostly fluctuated between approximately 0.5 to 2.5 m/s during the test period, except during the night hours of the third day (7:00 PM to 6:30 AM), where the wind speed fluctuated around zero. Thus, it can be said that an effective solar radiation budget was recorded, which might accelerate the heating of concrete during the day hours, while the moderately low wind speed might play a minimal role in cooling down this temperature increase within the first hours of concrete casting, especially when the effect of side wall insulation provided by wooden formwork is considered.

3.2 Variation of concrete temperatures with time

Figure 3 presents the time-dependent variation of concrete temperatures at the ten thermocouples together with air temperature (Ta). These thermocouples were presented in two subfigures to show the differences in responses of the two groups of thermocouples. The first group (Figure 3(a)) consists of the eight core thermocouples that are distributed along the mid-height section's centerline of the four walls, which were all installed 250 mm from the outer and inner surfaces, while the second group consists of one of the central thermocouples (SW) in addition to a corresponding exterior surface thermocouple and another interior surface thermocouple to form a section line along the south-west corner of the box-section, as shown in Figure 3(b).

It is seen in Figures 3(a) and (b) that despite the dropping of the air temperature after concrete casting (at 2:30 PM), the concrete temperature kept rising rapidly within the first 3 hours after concrete pouring, which reflects considerable heat release from cement hydration that counteracts the sinusoidal drop of air temperature within the late day hours related to the drop of solar radiation. During the first few hours after sunset, the concrete temperatures seem to be stabilized within their maximum range of approximately 61 to 65 ^{o}C, with the gap increasing between air temperature and concrete temperatures. The steep drop of air temperature during the night hours and until sunset slightly affected the temperature of concrete thermocouples due to the air convection cooling, directly on the top surface and indirectly across the side wooden walls, where the concrete temperature was fluctuating around approximately 58 ^{o}C. Similarly, starting from the early shining hours, the concrete temperature started to rise to recover the lost heat during the night hours and reach the 65 ^{o}C upper bound temperature of the previous day, showing a temperature increase of approximately 7 ^{o}C compared to the dawn time temperatures. Hence, the minor fluctuation of concrete temperature along late-night hours and second-day morning and noon hours reflects a minor effect of environmental thermal loads on concrete temperature behavior, which means that the heat of cement hydration is the controlling source during the full first 24 hours. The same minor effectiveness of solar radiation and air temperature remained during the early afternoon hours, while a sharp drop in concrete temperature started to be recorded after 3:00 PM on the next day, as shown in Figure 3, which might refer to the drop of heat release from cement hydration and the start of a new behavior where environmental loads are the dominant influencing factors. It is clear in Figure 3 that the behavior of concrete temperature became more strongly time-dependent and much more related to the sinusoidal variation of air temperature during the dark hours of the night and the sunny hours of the third day.

Differences between the different central thermocouples were generally insignificant as clearly shown in Figure 3(a), while more significant differences are shown in Figure 3(b) between the southwest's exterior surface and interior thermocouples, which is self-explanatory and directly related to their locations from the surfaces, where core temperatures reserve higher hydration heat compared to surface thermocouples. On the other hand, and the exterior surface thermocouple SWext is more affected by the air convection cooling through formwork compared to the core SW and interior surface SWint thermocouples, which explains its lower temperature during the late first day's hours and the following night hours. Oppositely, its temperature was the highest during the second day's noon hours

due to the higher received solar radiation intensity compared to SW and SWint. A minor but different effect of solar radiation is also clear in Figure 3(a) on the core thermocouples. As shown in the figure for the noon hours of the second day, SW exhibited the highest temperature due to its location with respect to the solar position at this time, where surfaces in this direction receive the highest solar radiation intensity. On the other hand, the northern wall's central thermocouple N recorded the lowest temperature because it was totally shaded during the whole preceding sunny hours.

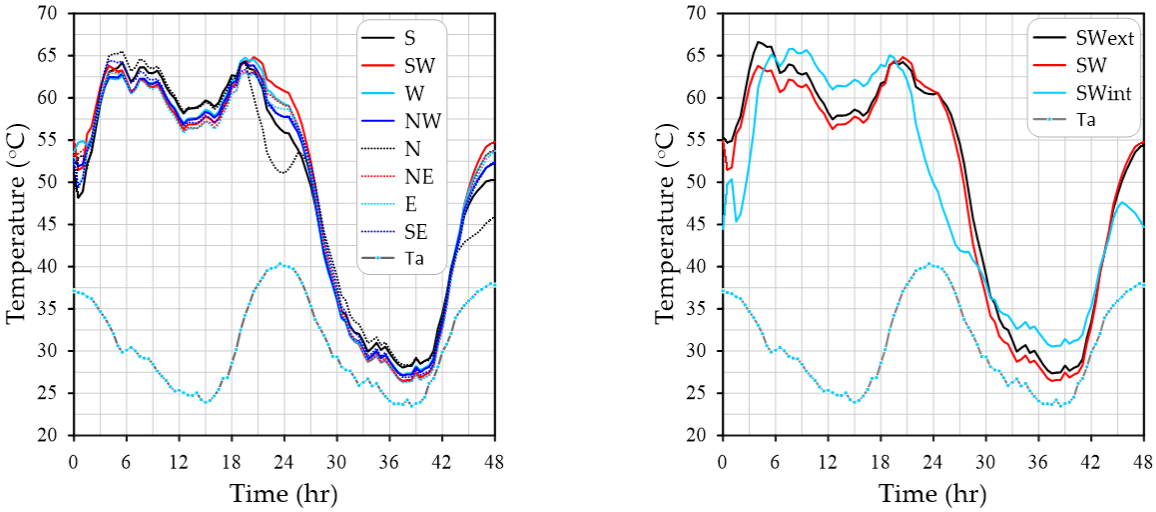

Figure 3. Hourly temperature variations of (a) core thermocouples (b) south-west section thermocouples

3.3 Concrete temperature differences

As discussed in the previous section, the concrete temperature became much more related to environmental thermal loads than to hydration heat within the last 12 hours of the first 48 hours. This means that the effect of hydration heat would be minimal and would diminish gradually over the following 24 hours, from 48 to 72 hours. Hence, the concrete temperatures are expected to be fully controlled by air temperature and solar radiation within the fourth day (from 72 to 96 hours) after concrete casting. Therefore, a comparison quantity similar to normalization was used to evaluate the extent and limits of the approximate sole cement hydration effect by excluding air temperature and solar radiation effects. This comparison quantity is termed the temperature difference and is calculated by subtracting the temperatures recorded from 72 to 96 hours from all temperatures recorded from time 0 to 48 hours. This procedure was conducted for the ten thermocouples as presented in Figure 4. Hence, for instance, the 48 temperature difference records of the S thermocouple along the first 24 hours ($T\text{-}T_{72\text{-}96}$) are the recorded temperatures of the thermocouple from 0 to 24 hours minus their corresponding records of the same thermocouple from 72 to 96 hours, and similarly, the temperature differences from 24 to 48 hours are those recorded during this period minus their corresponding records from 72 to 96 hours. The horizontal red line in the figures evaluates the air temperature differences that fluctuate around the zero value, while the vertical red line determines the time at which the concrete temperature differences approach zero, which declares zero effect of hydration heat.

As shown in Figure 4, it is clear that the temperature difference was slightly lower than that of the air temperature at casting time, where all thermocouples were recording the air temperature inside the cavity of formwork, which was less affected by the accumulated heating influence of solar radiation. After approximately one hour, the temperature difference started exhibiting three distinguishable stages with time. At the first stage, the temperature difference jumped rapidly, reaching approximately 32 ^{o}C after approximately 9 hours. Then, a second semi-stabilization stage was recorded from approximately 9 to 18 hours, where the temperature difference remained high and fluctuated

around 30 ºC. After 18 hours from concrete casting, the third sharp dropping stage started, where the temperature difference dropped from approximately 30 ºC to 3 ºC within 6 hours. The end of this stage can be considered as a second minor temperature difference stabilization zone, which extended another 6 hours under the effect of the noon and afternoon heating sunny hours of the second day. After approximately 30 hours, the temperature difference reached zero and started a fully-dependent fluctuation behavior similar to that of the air temperature difference. Thus, it can be concluded from Figure 4 that the minimal effect of hydration heat point was reached after 30 hours, which initiates the life-span status of full dependence on environmental thermal loads.

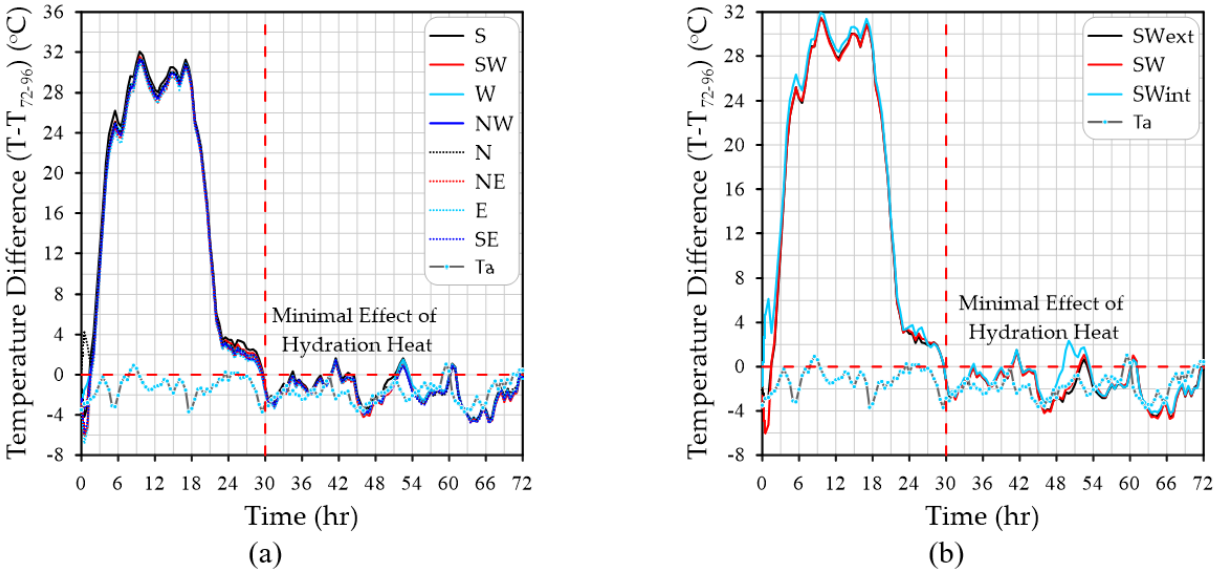

Figure 4. Hourly temperature differences (T-$T_{72\ to\ 96}$) (a) core thermocouples (b) south-west section thermocouples

The results of temperature differences are better presented in Figures 5 and 6, which show the maximum temperature difference records and minimum temperature difference records, respectively, for each thermocouple within intervals of 6 hours starting from the concrete casting time. For instance, the time 6 hours in Figure 5 represents the maximum temperature difference recorded for the first 6 hours (from 0 to 6), while the time 12 represents the maximum for the second 6 hours (from 6 to 12). These figures better highlight the temperature difference stabilization zone between 30 and 36 hours, where the maximum differences fluctuated around 0 ºC (Figure 5), while the minimum differences followed the air temperature trend (Figure 6).

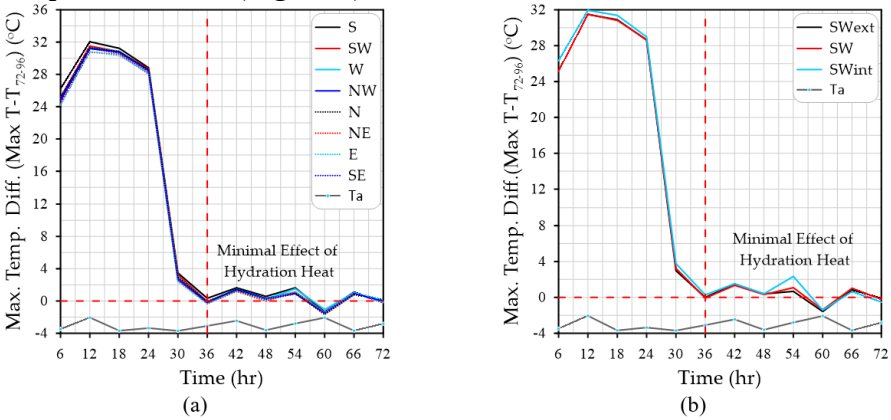

Figure 5. Maximum temperature differences (Max T-$T_{72\ to\ 96}$) for 6-hour intervals for (a) core thermocouples (b) south-west section thermocouples

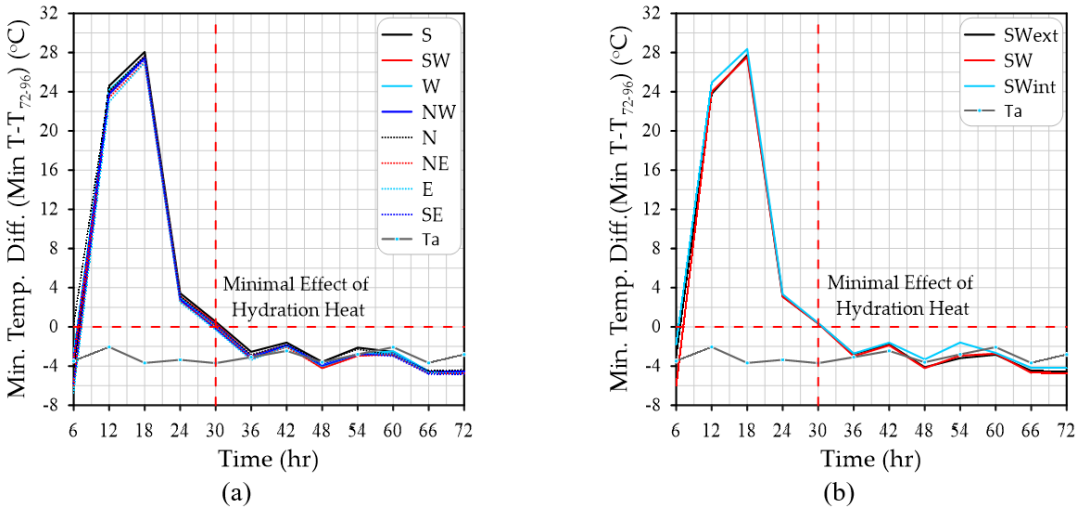

Figure 6. Minimum temperature differences (Min T-$T_{72\ to\ 96}$) for 6-hour intervals for (a) core thermocouples (b) south-west section thermocouples

The overall maximum 6-hour interval values of all thermocouples and the overall minimum 6-hour interval values of all thermocouples are depicted together in Figure 7. The figure clearly shows that the actual temperature difference stabilization starts after 36 hours from concrete casting. Another significant observation from the figure is that the maximum temperature difference was 32 ºC, while the temperature difference was generally higher than 26 ºC during the first 24 hours. If the air temperature difference between the first 48 hours and the 72-96 hours is considered, it can be said that the effect of hydration heat on concrete temperature during the first 24 hours was in the range of 30 to 35 ºC, where the fourth day (72 to 96 hours) was colder than the first day by approximately 3.5 ºC.

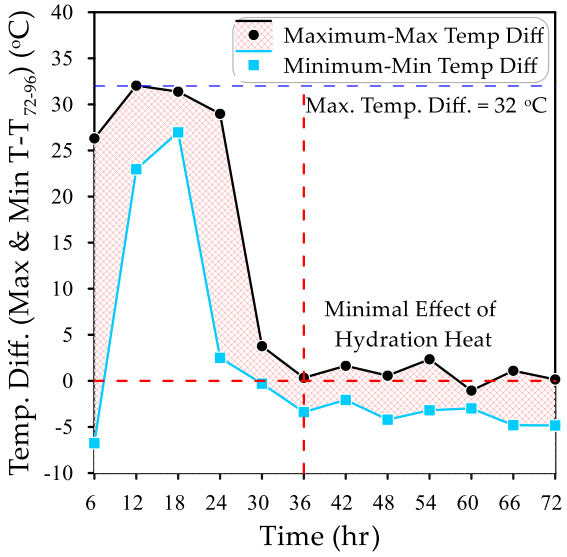

Figure 7. Overall maximum and minimum temperature differences (Max T-$T_{72\ to\ 96}$ and Min T-$T_{72\ to\ 96}$)

4. Conclusions

The following concluding remarks represent the most significant outputs of the experimental post-casting temperature measurements conducted in this study on a full-scale reinforced concrete box-segment:

1. Even though the temperature of all thermocouples was controlled by the heat of cement hydration, the exterior surface thermocouple revealed a greater sensitivity to atmospheric night cooling and day heating within the first 30 hours of concrete casting.
2. The temperature differences, which represent the differences between the temperature recorded by each of the 10 thermocouples during the first 48 hours after concrete casting, from their corresponding records after 72 to 96 hours, were used as a non-direct measurement tool to evaluate the individual effect of hydration heat on concrete temperature. The temperature differences reached approximately zero after 30 hours, which declares the point of minor effect of hydration heat on concrete temperature, and the start of the almost complete dependency on environmental thermal loads.
3. The 6-hour interval individual maximum and minimum records showed that the temperature difference stabilization zone lay between 30 and 36 hours after concrete casting, where the maximum differences fluctuated around 0 ^{o}C, while the minimum differences followed the air temperature difference trend.
4. The overall maximum of the 6-hour interval maximum records showed that the hydration heat was responsible for increasing the concrete temperature by approximately 26 to 32 ^{o}C during the first 24 hours, while this range increases to approximately 30 to 36 when the air temperature differences between the compared time intervals (first 24 hours and 72-96 hours) are considered.

Declaration of Competing Interest

The authors declare that there are no conflicts of interest regarding the publication of this manuscript.

Funding Information

No funding was received from any financial organization to conduct this research

Author Contributions

All authors effectively contributed to the work done and presented in this article. The experimental work was designed by Sallal R. Abid and conducted by Noora K. Jebur, including geometry, orientation, sensor instrumentation, data acquisition, and concrete casting. The experimental data were collected by Noora K. Jebur and analyzed by Sallal R. Abid and Mustafa Özakça. The three authors shared the verification and the discussion of the results, in addition to the writing of the original draft, while the presentation of figures and tables was done by Noora K. Jebur and Sallal R. Abid. Mustafa Özakça reviewed/edited the final copy of the article.

Acknowledgments

The authors express their gratitude to Wasit University/ College of Engineering/Civil Engineering Department in Kut city, Wasit, Iraq for supporting this study. In addition, the authors are thankful to Prof. Dr. Muhannad A. Shallal/Al-Qadisiyah University for his valuable technical support.

5. References

[1]. B. Klemczak. “Modeling Thermal-Shrinkage Stresses in Early Age Massive Concrete Structures - Comparative Study of Basic Models” ***Archives of Civil and Mechanical Engineering*** vol. 14, no.4, p.721-733, 2014.

[2] H. Abeka, S. Agyeman,M. Adom-Asamoah, “Thermal Effect of Mass Concrete Structures in the Tropics: Experimental, Modelling and Parametric Studies” ***Cogent Engineering*** vol. 4, no. 1, p. 1278297, 2017.

[3] G. W. William, S. N. Shoukry, M. Y. Raid. “Early Age Cracking of Reinforced Concrete Bridge Decks” ***Bridge Structures Assessment Design and Construction***, vol. 1, no.4, p. 379-396, 2005.

[4] D. P. Bentz, P. E. Stutzman, A. R. Sakulich, W. J. Weiss. “Study of Early-Age Bridge Deck Cracking in Nevada and Wyoming” ***National Institute of Standards and Technology: U.S. Department of Commerce***, vol. 100, no.56, p. 7841, 2012.

[5] A. D. Pofale, K. C. Tayade, N. V. Deshpande. “Calorimetric Studies on Heat Evolution and Temperature Rise Due to Hydration of Cementitious Materials in Concrete Using Semi-Adiabatic Calorimeter” ***International Journal of Application or Innovation in Engineering and Management RATMIEG 2013***, p. 1-7, 2013.

[6] K. A. Riding, J. L. Poole, K. J. Folliard, M. C. G. Juenger, and A. K. Schindler, “Modeling Hydration of Cementitious Systems” ***ACI Materials Journal***, vol. 109, no. 2, p. 51683709, 2012.

[7] S. G. Kim. “Effect of Heat Generation from Cement Hydration on Mass Concrete Placement” M.Sc. thesis, Iowa State University, Civil Engineering Department, p. 114, 2010.
[8] J. S. Du, X. F. Luo, P. L. Ng, and F. T. K. Au, “Early Age Temperature Rise and Thermal Stresses Induced in Concrete Bridge Pier,” ***Advanced Materials Research***, vol. 163, pp. 2731–2737, 2011.
[9] B. Chen, R. Ding, J. Zheng, and S. Zhang, “Field Test on Temperature Field and Thermal Stress for Prestressed Concrete Box-Girder Bridge,” ***Frontiers of Architecture and Civil Engineering in China***, vol. 3, no. 2, pp. 158–164, 2009.
[10] S. R. Abid, H. Atiya, N. Tayşi, M. Özakça. “Early Age Temperature Distributions in Reinforced Concrete Box- Girder”. 11th International Congress on Advances in Civil Engineering, ACE 2014 Oct 21-25; Istanbul, Turkey: p. 1-7, 2014.
[11] N. M. Laibi and M. A. Shallal, “Early Age Temperature Distributions in Concrete Bridge in the Middle of Iraq (Experimental Study)" ***Journal of Physics: Conference Series***, vol. 1895, no.1, p.012058, 2021.
[12] Z. Zhang, J. Liu, Y. Liu, Y. Lyu, B. Gong, Y. Ma, “Research on Hydration Heat Effect and Influence Parameters of Concrete-Filled Steel Shell Composite Pylon,” ***Structures***, vol. 70, p. 107860, 2024.
[13] B. T. Phung and T. C. Nguyen, “Temperature Field Determination during Bridge Pier Construction,” ***Engineering, Technology & Applied Science Research***, vol. 15, no. 2, pp. 20966–20971, 2025.